Quark model study of strange dibaryon resonances

Mei Chen, Hongxia Huang, and Jialun Ping*

Department of Physics, Nanjing Normal University, Nanjing 210097, People's Republic of China

Fan Wang

Department of Physics, Nanjing University, Nanjing 210093, People's Republic of China

(Received 4 October 2010; published 13 January 2011)

Two nonrelativistic quark models, a chiral quark model and a quark delocalization color screening model, are employed to calculate the baryon-baryon scattering phase shifts to look for dibaryon resonances with strangeness by means of the resonating group method. The two models predict similar-strangeness dibaryon resonance states. No resonance appears in the octet-octet channels, but resonance did exist in the octet-decuplet and decuplet-decuplet channels. These resonances were distributed in the energy region 2400–2800 MeV. The widths are generally smaller than 10 MeV but increased to tens of MeV after taking into account the off-shell widths of decuplet baryons. These resonances all appear in the D-wave nucleon-hyperon and hyperon-hyperon scatterings and can be searched for through hyperon-nucleon scatterings with hyperon beams and hyperon-hyperon vertex and masses reconstruction with the data collected by relativistic heavy ion collisions.

DOI: 10.1103/PhysRevC.83.015202 PACS number(s): 12.39.Jh, 13.75.Ev, 14.20.Pt

I. INTRODUCTION

Since Jaffe's prediction of the H particle [1], there have been big efforts, both theoretically and experimentally, to search for dibaryons [2]. In 1987, M. Oka *et al.* [3] claimed that a sharp resonance appears in $^1S_0$ $\Lambda\Lambda$ scattering at $E_{\mathrm{c.m.}} = 26.3$ MeV, which might correspond to the dihyperon state H particle. Moreover, M. Oka [4] also proposed several $J = 2^+$ dibaryons in the quark cluster model without meson exchange. In 1987, Goldman *et al.* proposed that the $S = -3$, $I = 1/2$, $J = 2$ dibaryon state might be a narrow resonance in a relativistic quark model [5]. The quark delocalization color screening model (QDCSM) confirmed that it was a very narrow resonance [6,7], whereas the chiral quark model claimed that $N\Omega$ and $\Delta\Omega$ systems are the weakly bound states [8]. In addition there are other dibaryon candidates, including the "inevitable" state $d^*(SIJ) = (003)$ [9], predicted in QDCSM [10,11]. In 1990, Kopeliovich *et al.* [12,13] predicted that there are strong-interaction-stable dibaryons with high strangeness, such as the $S = -6$ di-Ω state within the flavor SU(3) Skyrmion model. Zhang *et al.* [14] showed that the $\Omega\Omega$ dibaryon has large binding energy and small size and suggested searching for the di-Ω in relativistic heavy ion collisions. The chiral SU(3) quark model also suggested several dibaryon candidates [15]. However, so far no dibaryon has been confirmed by experiments. Recently, the CELSIUS-WASA Collaboration reported that the production cross section of the $pn \to d\pi^0\pi^0$ reaction shows evidence of an isoscalar $J^P = 1^+$ or 3^+ subthreshold $\Delta\Delta$ resonance with mass $\sim$2.36 GeV and width $\sim$80 MeV [16], which stimulates the research further. In addition, the recent experiments of the BaBar, Belle, and BES Collaborations also suggest the existence of tetraquark and baryonium systems [17–20]. The further experiments at COSY, JLab, BEPCII, SPRING-8, COMPAS, and other facilities will provide more information on exotic hadrons. Especially with the availability of strange hadron beams, J-PARC will be a good place to do hyperon-nucleon (YN) scattering to search for strange dibaryons.

Quantum chromodynamics (QCD) has been verified to be the fundamental theory of the strong interaction in the perturbative region. However, in the low-energy region, it is hard to directly use QCD to study complicated systems such as hadron-hadron interactions and exotic quark states due to their nonperturbative nature, although lattice QCD has made impressive progress on nucleon-nucleon (NN) interactions and tetra- and pentaquark systems [21–23]. Therefore, various QCD-inspired models have been developed to obtain physical insights into many phenomena of the hadronic world.

To study the baryon-baryon interaction, the most common approach is the chiral quark model (ChQM) [24,25], in which the constituent quarks interact with each other through Goldstone-boson exchange in addition to the effective one-gluon exchange. To obtain the immediate-range attraction, the σ meson has to be introduced. BES and other collaborations have observed a signal in $\pi\pi$ invariant mass spectra. But the modern treatments of correlated two-pion exchange show that in addition to a long-range scalar-isoscalar attraction traditionally associated with scalar exchange, there is also a strong scalar-isoscalar repulsive core [26], a complication that has not yet been included in the σ exchange.

An alternative approach to study baryon-baryon interaction is the QDCSM [27], which was developed in the 1990s with the aim of explaining the similarities between nuclear and molecular forces. By introducing the quark delocalization to enlarge the model space and taking into account the differences of confinement interaction inside a single baryon and between two color-singlet baryons, the model gives a good description of NN and YN interactions and the properties of deuteron [10,27,28]. Recent studies also show that the intermediate-range attraction mechanism in the QDCSM, quark

*Jlping@njnu.edu.cn

delocalization and color screening, is an alternative mechanism for the σ-meson exchange in the ChQM [29].

To provide the necessary information for experiments to search for the dibaryon states, dibaryon spectrum calculation alone is not enough. The calculation of baryon-baryon scattering, the main production process of dibaryons, is indispensable. The scattering phase shifts will show a resonance behavior in the dibaryon resonance energy region. The NN scattering phase shifts including $N\Delta$ and $\Delta\Delta$ channel couplings in the framework of the resonating group method (RGM) [30] have been calculated recently [31]. Extending the calculation to the strange sector is the goal of the present work. As before, two quark models, ChQM and QDCSM, are used for a mutual check.

In the RGM equation, the reduced mass of two clusters is obtained by separating the total kinetic energy of six quarks into an internal part, a relative motion part, and a center-of-mass part. For NN scattering, the theoretical reduced mass is the same as the experimental one. For strange baryons, the theoretical reduced masses are different from the experimental ones. To ensure the correct scattering kinematics, the reduced mass employed in the RGM equation should be, therefore, readjusted to the experimental value. A prescription to do this without breaking the Pauli principle is used and will be discussed in detail in Sec. II. In addition, a brief description of the QDCSM and the ChQM is also given in Sec. II. In Sec. III, we present calculated results and a discussion. Finally, a summary is given Sec. IV.

II. TWO QUARK MODELS AND MODIFICATION OF THE RESONATING GROUP EQUATION

A. Chiral quark model

In the chiral quark model, the constituent quarks acquire their masses due to the spontaneous breaking of chiral symmetry. These quasiparticles interact with each other through Goldstone-boson π, K, η exchange, in addition to the effective one-gluon exchange from QCD dynamics (perturbative part). The color confinement is imitated by the confining potential, which is usually simplified to be quadratically dependent on the interquark distance. The model details can be found in Refs. [32,33]. Here we only give the Hamiltonian:

$$H = \sum_{i=1}^{6}\left(m_i + \frac{p_i^2}{2m_i}\right) - T_{\rm c.m.} + \sum_{j>i=1}^{6}\left(V_{ij}^C + V_{ij}^G + V_{ij}^\chi + V_{ij}^\sigma\right), \quad (1)$$

$$V_{ij}^C = -a_c \boldsymbol{\lambda}_i^c \boldsymbol{\lambda}_j^c ({r_{ij}}^2 + v_0), \quad (2)$$

$$V_{ij}^G = \frac{1}{4}\alpha_s \boldsymbol{\lambda}_i^c \boldsymbol{\lambda}_j^c \left[\frac{1}{r_{ij}} - \frac{\pi}{2}\delta(\boldsymbol{r}_{ij})\left(\frac{1}{m_i^2} + \frac{1}{m_j^2} + \frac{4\boldsymbol{\sigma}_i\boldsymbol{\sigma}_j}{3m_i m_j}\right) - \frac{3}{4m_i m_j r_{ij}^3} S_{ij}\right], \quad (3)$$

$$V_{ij}^\chi = V_\pi(\boldsymbol{r}_{ij})\sum_{a=1}^{3}\lambda_i^a\lambda_j^a + V_K(\boldsymbol{r}_{ij})\sum_{a=4}^{7}\lambda_i^a\lambda_j^a + V_\eta(\boldsymbol{r}_{ij})\left[\left(\lambda_i^8\lambda_j^8\right)\cos\theta_P - \left(\lambda_i^0\lambda_j^0\right)\sin\theta_P\right], \quad (4)$$

$$V_\chi(\boldsymbol{r}_{ij}) = \frac{g_{\rm ch}^2}{4\pi}\frac{m_\chi^2}{12m_i m_j}\frac{\Lambda_\chi^2}{\Lambda_\chi^2 - m_\chi^2}m_\chi\left\{(\boldsymbol{\sigma}_i\boldsymbol{\sigma}_j)\left[Y(m_\chi r_{ij}) - \frac{\Lambda_\chi^3}{m_\chi^3}Y(\Lambda_\chi r_{ij})\right] + \left[H(m_\chi r_{ij}) - \frac{\Lambda_\chi^3}{m_\chi^3}H(\Lambda_\chi r_{ij})\right]S_{ij}\right\}, \quad \chi = \pi, K, \eta, \quad (5)$$

$$V_\sigma(\boldsymbol{r}_{ij}) = -\frac{g_{\rm ch}^2}{4\pi}\frac{\Lambda_\sigma^2}{\Lambda_\sigma^2 - m_\sigma^2}m_\sigma\left[Y(m_\sigma r_{ij}) - \frac{\Lambda_\sigma}{m_\sigma}Y(\Lambda_\sigma r_{ij})\right], \quad (6)$$

$$S_{ij} = \left\{3\frac{(\boldsymbol{\sigma}_i\boldsymbol{r}_{ij})(\boldsymbol{\sigma}_j\boldsymbol{r}_{ij})}{r_{ij}^2} - \boldsymbol{\sigma}_i\boldsymbol{\sigma}_j\right\}, \quad (7)$$

$$H(x) = (1 + 3/x + 3/x^2)Y(x), \quad Y(x) = e^{-x}/x, \quad (8)$$

where α_s is the quark-gluon coupling constant. In order to cover the wide energy range from light, strange, to heavy quarks one introduces an effective scale-dependent quark-gluon coupling constant $\alpha_s(\mu)$ [34]:

$$\alpha_s(\mu) = \frac{\alpha_0}{\ln\left(\frac{\mu^2+\mu_0^2}{\Lambda_0^2}\right)}. \quad (9)$$

The coupling constant $g_{\rm ch}$ for a scalar chiral field is determined from the $NN\pi$ coupling constant through

$$\frac{g_{\rm ch}^2}{4\pi} = \left(\frac{3}{5}\right)^2\frac{g_{\pi NN}^2}{4\pi}\frac{m_{u,d}^2}{m_N^2}, \quad (10)$$

and flavor SU(3) symmetry is assumed. The other symbols in these expressions have their usual meanings.

B. Quark delocalization color screening model

The Hamiltonian of the QDCSM is the same as that of the chiral quark model but with two modifications [10,11,27]: First, there is no σ-meson exchange in the QDCSM, and second, the screened color confinement is used between quark pairs that reside in different baryon orbits. That is,

$$V_{ij}^C = \begin{cases} -a_c \boldsymbol{\lambda}_i^c \boldsymbol{\lambda}_j^c \left(r_{ij}^2 + v_0\right) & \text{if } i,j \text{ is in the same baryon orbit,} \\ -a_c \boldsymbol{\lambda}_i^c \boldsymbol{\lambda}_j^c \left(\frac{1-e^{-\mu_{ij}\mathbf{r}_{ij}^2}}{\mu_{ij}} + v_0\right) & \text{otherwise.} \end{cases} \tag{11}$$

The color screening constant μ_{ij} in Eq. (11) is determined by fitting the deuteron properties, NN scattering phase shifts, and $N\Lambda$ and $N\Sigma$ scattering cross sections, respectively, $\mu_{uu} = 1.20$, $\mu_{us} = 0.30$, and $\mu_{ss} = 0.08$, satisfying the relation $\mu_{us}^2 = \mu_{uu}\mu_{ss}$.

The quark delocalization in the QDCSM is realized by replacing the left- (right-) centered single Gaussian functions, the single-particle orbital wave function in the usual quark cluster model,

$$\begin{aligned} \phi_\alpha(\boldsymbol{S}_i) &= \left(\frac{1}{\pi b^2}\right)^{\frac{3}{4}} e^{-\frac{(r-S_i/2)^2}{2b^2}}, \\ \phi_\beta(-\boldsymbol{S}_i) &= \left(\frac{1}{\pi b^2}\right)^{\frac{3}{4}} e^{-\frac{(r+S_i/2)^2}{2b^2}} \end{aligned} \tag{12}$$

with delocalized ones,

$$\begin{aligned} \psi_\alpha(\boldsymbol{S}_i, \epsilon) &= [\phi_\alpha(\boldsymbol{S}_i) + \epsilon\phi_\alpha(-\boldsymbol{S}_i)]/N(\epsilon), \\ \psi_\beta(-\boldsymbol{S}_i, \epsilon) &= [\phi_\beta(-\boldsymbol{S}_i) + \epsilon\phi_\beta(\boldsymbol{S}_i)]/N(\epsilon), \\ N(\epsilon) &= \sqrt{1 + \epsilon^2 + 2\epsilon e^{-S_i^2/4b^2}}. \end{aligned} \tag{13}$$

The delocalization parameter $\epsilon(\boldsymbol{S}_i)$ is determined by the dynamics of the quark system rather than adjusted parameters. In this way, the system can choose its most favorable configuration through its own dynamics in a larger Hilbert space.

The parameters of the two models are given in Table I. The calculated baryon masses in comparison with experimental values are shown in Table II.

TABLE I. The parameters of the two models studied: $m_\pi = 0.7$ fm^{-1}, $m_k = 2.51$ fm^{-1}, $m_\eta = 2.77$ fm^{-1}, $m_\sigma = 3.42$ fm^{-1}; $\Lambda_\pi = 4.2$ fm^{-1}, $\Lambda_k = 5.2$ fm^{-1}, $\Lambda_\eta = 5.2$ fm^{-1}, $\Lambda_\sigma = 4.2$ fm^{-1}; $g_{ch}^2/(4\pi) = 0.54$; $\theta_p = -15°$.

Model		QDCSM	ChQM
State	b (fm)	0.6	0.518
	m_u (MeV)	313	313
	m_d (MeV)	313	313
	m_s (MeV)	539	573
Confinement	a_c (MeV)	18.5283	48.59
	μ_{uu}	1.20	–
	μ_{us}	0.30	–
	μ_{ss}	0.08	–
	v_0 (MeV)	−0.3333	−1.2145
OGE	α_0	0.7089	0.5101
	Λ_0 (fm^{-1})	1.7225	1.5250
	μ_0 (MeV)	445.8512	445.8080

TABLE II. The masses of ground-state baryons (in MeV).

	N	Δ	Λ	Σ	Σ^*	Ξ	Ξ^*	Ω
QDCSM	939	1232	1118	1224	1358	1365	1499	1654
ChQM	939	1232	1124	1238	1360	1374	1496	1642
Expt.	939	1232	1116	1193	1385	1318	1533	1672

C. The calculation method

To calculate the baryon-baryon scattering phase shifts, the well-developed RGM is used. The details of the RGM can be found in Refs. [30,31]. Here only the necessary equations and the appropriate treatment of the reduced mass of two baryons are given. In the RGM, the multiquark wave function is approximated by the cluster wave function

$$\psi(\boldsymbol{\xi}_1, \boldsymbol{\xi}_2, \boldsymbol{R}) = \mathcal{A}\phi(\boldsymbol{\xi}_1)\phi(\boldsymbol{\xi}_2)\chi(\boldsymbol{R}),$$

where $\boldsymbol{\xi}_i, i = 1, 2$ are the internal coordinates of quark cluster 1 and 2 and $\boldsymbol{R}$ is the coordinate of the relative motion of two quark clusters. The internal motions of clusters are frozen, and the relative motion wave function $\chi(\boldsymbol{R})$ satisfies the following RGM equation:

$$\int H(\boldsymbol{R}'', \boldsymbol{R}')\chi(\boldsymbol{R}')\,d\boldsymbol{R}' = E\int N(\boldsymbol{R}'', \boldsymbol{R}')\chi(\boldsymbol{R}')\,d\boldsymbol{R}', \tag{14}$$

where

$$\left\{\begin{matrix} H(\boldsymbol{R}'', \boldsymbol{R}') \\ N(\boldsymbol{R}'', \boldsymbol{R}') \end{matrix}\right\} = \Big\langle \mathcal{A}[\phi_1\phi_2\delta(\boldsymbol{R} - \boldsymbol{R}'')] \times \left|\left\{\begin{matrix} H \\ 1 \end{matrix}\right\}\right| \mathcal{A}[\phi_1\phi_2\delta(\boldsymbol{R} - \boldsymbol{R}')]\Big\rangle. \tag{15}$$

$\mathcal{A} = 1 + \mathcal{A}'$ is the antisymmetrization operator and has the properties $\mathcal{A}H = H\mathcal{A}$, $\mathcal{A}^2 = \mathcal{A}$. With these properties, the RGM equation can be written as an integrodifferential equation:

$$\left[\frac{\nabla_{R''}^2}{2\mu} - V^D(\boldsymbol{R}'') + E_{\text{c.m.}}\right]\chi(\boldsymbol{R}'') = \int W_L(\boldsymbol{R}'', \boldsymbol{R}')\chi(\boldsymbol{R}')\,d\boldsymbol{R}', \tag{16}$$

where $E_{\text{c.m.}} = E - E_{\text{int}}$ is the kinetic energy of the relative motion, and W_L is the whole exchange kernel,

$$W_L(\boldsymbol{R}'', \boldsymbol{R}') = H^E(\boldsymbol{R}'', \boldsymbol{R}') - EN^E(\boldsymbol{R}'', \boldsymbol{R}'), \tag{17}$$

where the exchange kernels of Hamiltonian and overlap are defined as

$$\begin{aligned} H^E(\boldsymbol{R}'', \boldsymbol{R}') &= \langle\phi_1\phi_2\delta(\boldsymbol{R} - \boldsymbol{R}'')|H|\mathcal{A}'[\phi_1\phi_2\delta(\boldsymbol{R} - \boldsymbol{R}')]\rangle, \\ N^E(\boldsymbol{R}'', \boldsymbol{R}') &= \langle\phi_1\phi_2\delta(\boldsymbol{R} - \boldsymbol{R}'')|\mathcal{A}'|\phi_1\phi_2\delta(\boldsymbol{R} - \boldsymbol{R}')\rangle. \end{aligned} \tag{18}$$

In Eq. (16), the reduced mass μ, which is obtained by decomposing the kinetic energies of six quarks into internal relative motion and center-of-mass parts, is generally not the same as the experimental one, which is the reduced mass of two baryons. In order to fit to the scattering kinematics, a prescription [35] has to be introduced, i.e., multiplying all the kinetic terms in Eq. (16) by μ/μ_{exp}, with μ_{exp} being the experimental reduced mass, and defining the physical relative motion energy

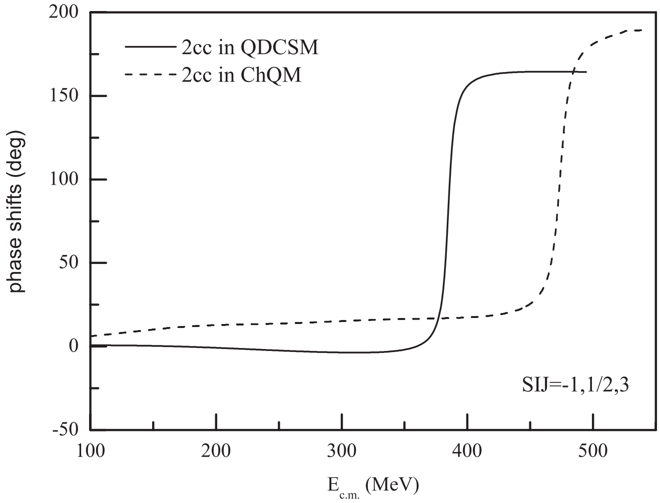

FIG. 1. The $N\Lambda$ D-wave phase shifts with $I, J = 1/2, 3$. 2cc represents $\Delta\Sigma^*$ and $N\Lambda$ channel coupling.

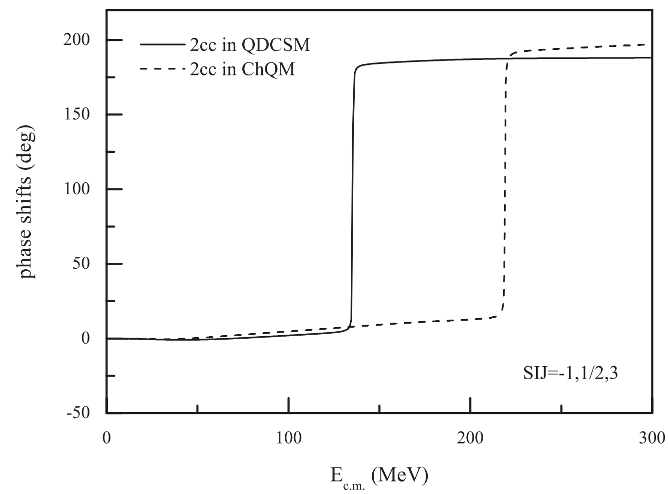

FIG. 3. The $N\Sigma^*$ D-wave phase shifts with $I, J = 1/2, 3$. 2cc represents $\Delta\Sigma^*$ and $N\Sigma^*$ channel coupling.

$\widetilde{E}_{\text{c.m.}}$ as $E - E_{\text{int}}^{\text{exp}}$, with $E_{\text{int}}^{\text{exp}}$ as the sum of two experimental masses of two baryons. Then the RGM equation to be solved is

$$\left[\frac{\nabla^2_{R''}}{2\mu_{exp}} - V^D(\boldsymbol{R}'') + \widetilde{E}_{c.m.}\right]\chi(\boldsymbol{R}'') = \int \widetilde{W}_L(\boldsymbol{R}'', \boldsymbol{R}')\chi(\boldsymbol{R}')\, d\boldsymbol{R}', \tag{19}$$

where $\widetilde{W}_L$ means that the kinetic kernel in it is multiplied by the factor μ/μ_{exp}.

III. RESULTS AND DISCUSSION

The baryon-baryon scattering that is accessible through experiments requires that the baryons are strong-interaction-stable baryons, i.e., octet baryons and Ω. So in the present calculation, the baryons in the initial state of scattering are limited to octet baryons and Ω. Two quark models have been successfully applied to describe the YN scattering cross sections [27,35]. In this work, we extend the calculation to other baryon channels. From the previous bound-state calculation [36], there is no octet-octet dibaryon state in the two quark models used here, and there are several octet-decuplet and decuplet-decuplet dibaryons. These dibaryons should appear as resonances in the corresponding octet-octet baryons' S- or D-wave scattering channels and acquire finite widths. In addition, the off-shell widths of decuplet baryons should also be considered if they are included in the dibaryon resonances. A simple estimation of the off-shell width for the bound unstable baryons is used in this calculation [31].

Among all channels calculated in this paper, the two models give essentially consistent results. In some sense, the results are not dependent on the details of models, and it also serves as a further test of the equivalence of two mechanisms for intermediate-range attraction. The general features of the calculated results are as follows. First, in the S-wave baryon-baryon scattering, there is no resonance occurring, similar to NN scattering. To save space, the detailed results of S-wave baryon-baryon scattering are not shown in this paper. Second, coupling to open D-wave baryon-baryon channels, the energies of bound states are pushed down a little, which means that the mass shift of the bound state is dominated by the open D-wave scattering states above the energy of the stand-alone bound state. The results are different from

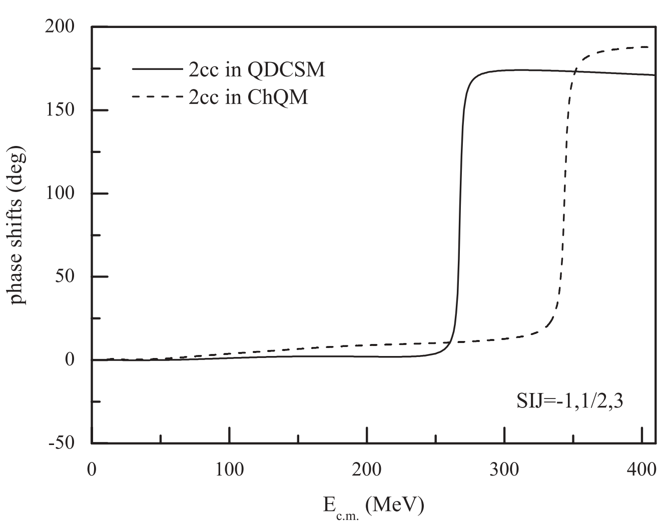

FIG. 2. The $N\Sigma$ D-wave phase shifts with $I, J = 1/2, 3$. 2cc represents $\Delta\Sigma^*$ and $N\Sigma$ channel coupling.

TABLE III. The masses and widths of state $S, I, J = -1, 1/2, 3$ in MeV. Γ_{bs} is the width contributed by decuplet baryons Δ and Σ^* in the bound state. The threshold of $\Delta\Sigma^*$ is 2617 MeV.

Coupled channels	QDCSM			ChQM		
	M	Γ	Γ_{bs}	M	Γ	Γ_{bs}
$\Delta\Sigma^*$	2446	–	–	2539	–	–
$\Delta\Sigma^*$-$N\Lambda$	2444	8.1	36.5	2538	12.2	101.0
$\Delta\Sigma^*$-$N\Sigma$	2444	3.2	31.6	2538	4.9	88.3
$\Delta\Sigma^*$-$N\Sigma^*$	2444	0.2	32.2	2538	0.5	78.9

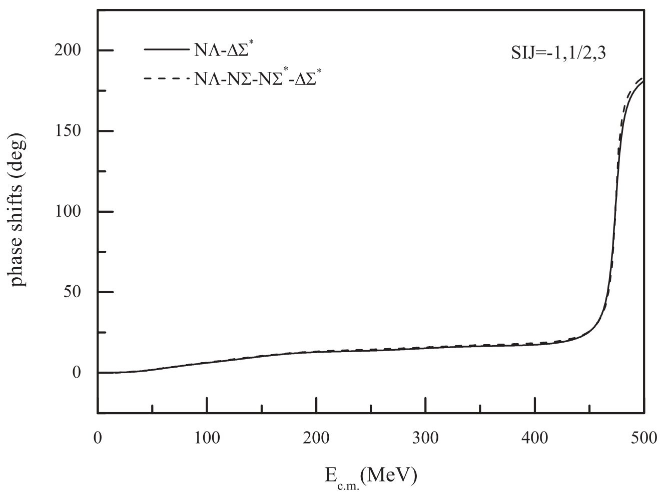

FIG. 4. The $N\Lambda$ D-wave phase shifts with $I, J = 1/2, 3$.

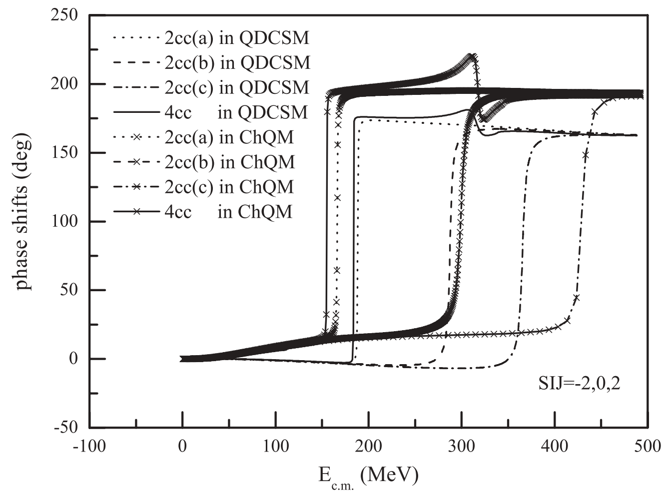

FIG. 5. The $\Lambda\Lambda$ D-wave phase shifts with $I, J = 0, 2$. 2cc(a), 2cc(b), and 2cc(c) stand for $\Lambda\Lambda$ coupling to $N\Xi^*$, $\Sigma\Sigma^*$, and $\Sigma^*\Sigma^*$, respectively. The four-channels coupling is denoted by 4cc.

those of NN scattering [31]. Third, the S-wave bound states decay to open D-wave baryon-baryon channels only through tensor interaction, so the decaying widths are generally small. However, the off-shell widths of decuplet baryons will greatly increase the total width of the dibaryon candidates. Here a simple formula [31,37] is used to calculate the off-shell widths of decuplet baryons. To do a systematic search of dibaryons, a crude estimate of the width of the dibaryon states is enough. To take into account the dynamical effect of the unstable particles in RGM, some serious prescriptions [38] should be used; these are left for further study. In the following, we present the results in order of increasing strangeness.

(i) $S = -1$. The state $\Delta\Sigma^*$ $(I, J = 1/2, 3)$ is a good dibaryon candidate with large binding energy in the two quark models. The possible decay channels are $N\Lambda$, $N\Sigma$, $N\Sigma^*$, and $\Delta\Sigma$. Because the mass of the dibaryon is lower than the threshold of $\Delta\Sigma$, the process $\Delta\Sigma^* \to \Delta\Sigma$ is forbidden. To find the width of the dibaryon, we calculate the scattering phase shifts of various possible scattering channels coupling to $\Delta\Sigma^*$.

Figures 1–3 show the results, and Table III gives the energy shifts and the decay widths of the dibaryon. The phase shifts clearly show a narrow resonance. Figure 1 shows the D-wave phase shifts of $N\Lambda$ scattering. From the shape of the resonance, the mass and the decay width of the dibaryon are obtained as 2444 and 8 MeV in the QDCSM and 2538 and 12 MeV in the ChQM. The small width is obviously due to tensor coupling. In comparison with the single $\Delta\Sigma^*$ channel calculation, the mass of the dibaryon is pushed down a little bit (1–2 MeV). Figures 2 and 3 show the D-wave phase shifts of $N\Sigma$ and $N\Sigma^*$ scattering, respectively. The locations of the resonance are the same as those of $N\Lambda$ scattering. Summing up the three scattering channel results, one finds that the decay width of this dibaryon is about 11 MeV in the QDCSM or 17 MeV in the ChQM. By taking into account the off-shell width Γ_{bs} of Δ and Σ^* themselves [31,37], the total width of this dibaryon is 48 MeV in the QDCSM or 118 MeV in the ChQM

TABLE IV. The mass and width of state $S, I, J = -2, 0, 2$ in MeV. Γ_{bs} is the width contributed by the decuplet baryons in the bound state. The thresholds of the three channels $N\Xi^*$, $\Sigma\Sigma^*$, and $\Sigma^*\Sigma^*$ are 2472, 2578, and 2770 MeV, respectively.

Coupling channels	QDCSM			ChQM		
	M	Γ	Γ_{bs}	M	Γ	Γ_{bs}
$N\Xi^*$	2430	–	–	2418	–	
$\Sigma\Sigma^*$	2531	–	–	2553	–	
$\Sigma^*\Sigma^*$	2611	–	–	2685	–	
$N\Xi^*$-$\Sigma\Sigma^*$-$\Sigma^*\Sigma^*$	2425	–	–	2407	–	
$N\Xi^*$-$\Lambda\Lambda$	2428	0.5	8.3	2416	1.0	7.4
$\Sigma\Sigma^*$-$\Lambda\Lambda$	2531	0.01	23.0	2551	9.0	24.5
$\Sigma^*\Sigma^*$-$\Lambda\Lambda$	2610	6.0	23.6	2683	8.7	53.0
$N\Xi^*$-$\Sigma\Sigma^*$-$\Sigma^*\Sigma^*$-$\Lambda\Lambda$	2424	0.1	7.7	2407	0.3	6.5
$N\Xi^*$-$N\Xi$	2429	3.8	8.5	2416	3.9	7.5
$\Sigma\Sigma^*$-$N\Xi$	2531	0.04	23.5	2552	0.2	25.5
$\Sigma^*\Sigma^*$-$N\Xi$	2610	2.5	24.2	2683	2.2	55.0
$N\Xi^*$-$\Sigma\Sigma^*$-$\Sigma^*\Sigma^*$-$N\Xi$	2423	3.3	7.9	2404	2.8	6.2

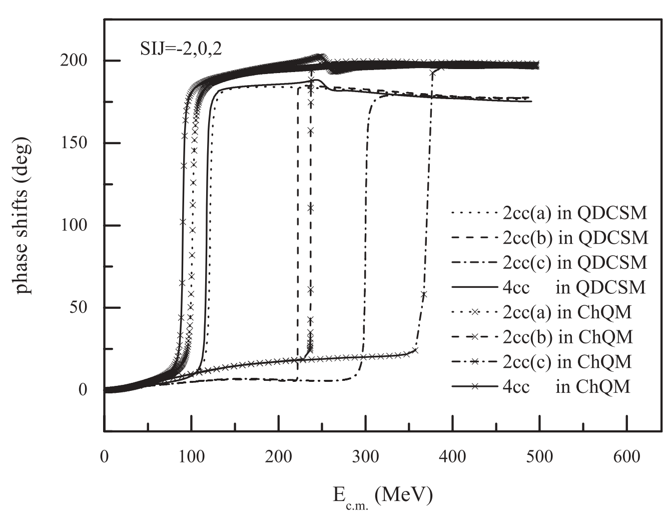

FIG. 6. The $N\Xi$ D-wave phase shifts with $I, J = 0, 2$. 2cc(a), 2cc(b), and 2cc(c) stand for $N\Xi$ coupling to $N\Xi^*$, $\Sigma\Sigma^*$, and $\Sigma^*\Sigma^*$, respectively. The four-channel coupling is denoted by 4cc.

TABLE V. The mass and width of state $S, I, J = -2, 1, 3$ in MeV. The theoretical thresholds of the two channels $\Delta\Xi^*$ and $\Sigma^*\Sigma^*$ are 2765 and 2770 MeV, respectively.

Coupling channels	QDCSM			ChQM		
	M	Γ	Γ_{bs}	M	Γ	Γ_{bs}
$\Delta\Xi^*$	2642	–	–	2702	–	–
$\Sigma^*\Sigma^*$	2647	–	–	nb[a]	–	–
$\Delta\Xi^*$-$\Sigma^*\Sigma^*$	2629	–	–	2662	–	–
$\Delta\Xi^*$-$N\Xi$	2642	0.01	55.2	2700	6.3	101.9
$\Sigma^*\Sigma^*$-$N\Xi$	2645	3.8	37.6	nr[b]	–	–
$\Delta\Xi^*$-$\Sigma^*\Sigma^*$-$N\Xi$	2627	2.4	47.5	2661	7.8	72.6
$\Delta\Xi^*$-$N\Xi^*$	2641	0.3	52.7	2701	0.5	96.6
$\Sigma^*\Sigma^*$-$N\Xi^*$	2646	0.08	36.0	nr	–	–
$\Delta\Xi^*$-$\Sigma^*\Sigma^*$-$N\Xi^*$	2628	0.2	45.5	2662	0.3	68.7
$\Delta\Xi^*$-$\Delta\Xi$	2642	0.08	55.0	2701	0.3	93.0
$\Sigma^*\Sigma^*$-$\Delta\Xi$	2646	0.02	37.0	nr	–	–
$\Delta\Xi^*$-$\Sigma^*\Sigma^*$-$\Delta\Xi$	2628	0.03	48.5	2662	0.1	69.8
$\Delta\Xi^*$-$\Sigma\Sigma$	2641	0.3	47.5	2701	0.4	86.3
$\Sigma^*\Sigma^*$-$\Sigma\Sigma$	2646	0.04	31.8	nr	–	–
$\Delta\Xi^*$-$\Sigma^*\Sigma^*$-$\Sigma\Sigma$	2628	0.2	41.6	2662	0.2	62.1
$\Delta\Xi^*$-$\Lambda\Sigma$	2641	3.5	47.6	2701	3.3	88.2
$\Sigma^*\Sigma^*$-$\Lambda\Sigma$	2645	0.06	31.8	nr	–	–
$\Delta\Xi^*$-$\Sigma^*\Sigma^*$-$\Lambda\Sigma$	2628	4.7	41.7	2661	6.6	62.1
$\Delta\Xi^*$-$\Sigma\Sigma^*$	2642	0.002	53.8	2701	0.011	92.8
$\Sigma^*\Sigma^*$-$\Sigma\Sigma^*$	2647	0.02	36.1	nr	–	–
$\Delta\Xi^*$-$\Sigma^*\Sigma^*$-$\Sigma\Sigma^*$	2628	0.0006	47.6	2662	0.002	68.5

[a]Unbound.
[b]No resonance in these coupled channels.

(taking the largest Γ_{bs}). The large width in ChQM is due to the small binding energy of the dibaryon with respect to the theoretical threshold of 2617 MeV. Coupling all these channels, $\Delta\Sigma^*$, $N\Lambda$, $N\Sigma$, and $N\Sigma^*$, we get almost the same results as those of the $\Delta\Sigma^*$-$N\Lambda$ channel coupling (see Fig 4).

J-PARC will have its Λ beam soon, and a ΛN scattering extending to this resonance energy region is expected.

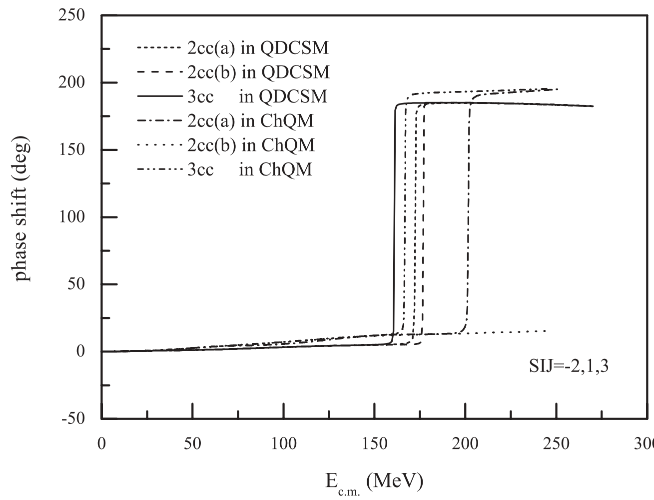

FIG. 8. The D-wave $\Sigma\Sigma$ phase shifts with $I, J = 1, 3$. 2cc(a) and 2cc(b) stand for $\Sigma\Sigma$ coupling to $\Delta\Xi^*$ and $\Sigma^*\Sigma^*$, respectively, and the three-channel coupling is denoted by 3cc.

Because the octet-decuplet baryon (except for Ω) scattering is not accessible, in the following we do not present the figures for octet-decuplet baryon scattering.

(ii) $S = -2$. The promising dibaryon candidate is the state with quantum numbers $I, J = 0, 2$. The state includes three channels, $N\Xi^*$, $\Sigma\Sigma^*$, and $\Sigma^*\Sigma^*$. Table IV gives some information about this state. According to its quantum numbers, this state can couple to octet-octet baryon channels $\Sigma\Sigma$, $\Lambda\Lambda$, and $N\Xi$ by tensor interaction. Because the mass of the dibaryon is lower than the $\Sigma\Sigma$ threshold, the decay to $\Sigma\Sigma$ is excluded. The D-wave scattering phase shifts of the $\Lambda\Lambda$ and $N\Xi$ channels are shown in Figs. 5 and 6, respectively. In the QDCSM, the $N\Xi^*$ single-channel calculation gives a bound-state mass of 2430 MeV, which is below the $N\Xi^*$ threshold. Coupling to the open D-wave $\Lambda\Lambda$ channel pushes the state down to 2428 MeV with a narrow width of 0.5 MeV. Similarly, $\Sigma\Sigma^*$ or $\Sigma^*\Sigma^*$ appears as a resonance in the $\Lambda\Lambda$

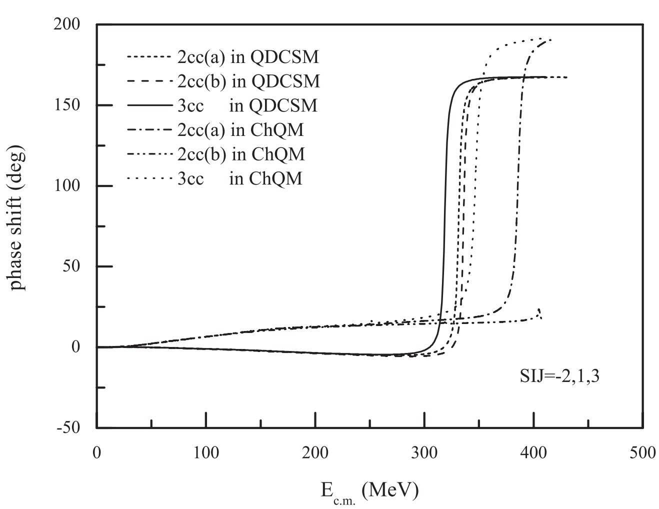

FIG. 7. The D-wave $N\Xi$ phase shifts with $I, J = 1, 3$. 2cc(a) and 2cc(b) stand for $N\Xi$ coupling to $\Delta\Xi^*$ and $\Sigma^*\Sigma^*$, respectively, and the three-channel coupling is denoted by 3cc.

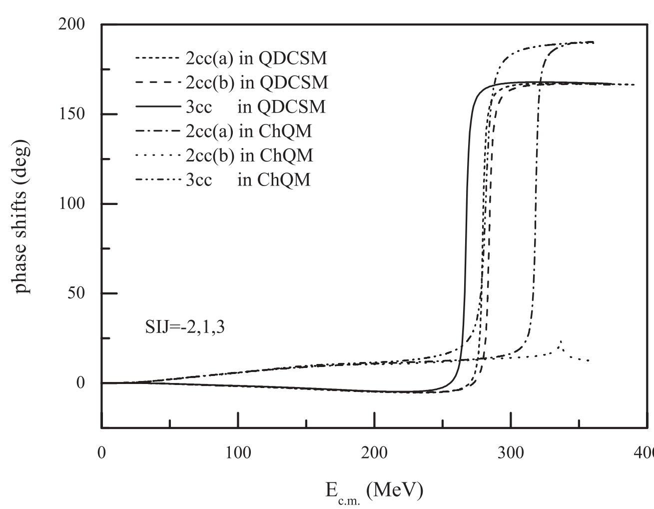

FIG. 9. The D-wave $\Lambda\Sigma$ phase shifts with $I, J = 1, 3$. 2cc(a) and 2cc(b) stand for $\Lambda\Sigma$ coupling to $\Delta\Xi^*$ and $\Sigma^*\Sigma^*$, respectively, and the three-channel coupling is denoted by 3cc.

TABLE VI. The mass and width of state $S, I, J = -3, 1/2, 2$ in MeV. The theoretical thresholds of the five channels $N\Omega$, $\Sigma\Xi^*$, $\Xi\Sigma^*$, $\Lambda\Xi^*$, and $\Sigma^*\Xi^*$ are 2611, 2726, 2703, 2649, and 2918 MeV, respectively.

Coupling channels	QDCSM			ChQM		
	M	Γ	Γ_{bs}	M	Γ	Γ_{bs}
$\Sigma\Xi^*$	2722	–	–	2724	–	–
$\Xi\Sigma^*$	2697	–	–	2712	–	–
$\Lambda\Xi^*$	nb[a]	–	–	2619	–	–
$\Sigma^*\Xi^*$	2802	–	–	2813	–	–
$N\Omega$	nb	–	–	2558	–	–
$N\Omega$-$\Sigma\Xi^*$-$\Xi\Sigma^*$-$\Lambda\Xi^*$- $\Sigma^*\Xi^*$	2549	–	–	2528	–	–
$\Sigma\Xi^*$-$\Lambda\Xi$	2721	1.7	8.9	2722	5.9	7.9
$\Xi\Sigma^*$-$\Lambda\Xi$	2696	1.0	29.0	2707	1.7	30.1
$\Lambda\Xi^*$-$\Lambda\Xi$	nr[b]	–	–	2619	0.2	9.6
$\Sigma^*\Xi^*$-$\Lambda\Xi$	2802	4.4	24.6	2510	8.5	28.9
$N\Omega$-$\Lambda\Xi$	2592	0.01	0.0	2557	0.2	0.0
$N\Omega$-$\Sigma\Xi^*$-$\Xi\Sigma^*$-$\Lambda\Xi^*$- $\Sigma^*\Xi^*$-$\Lambda\Xi$	2547	0.004	3.9	2528	0.1	1.7

[a]Unbound.
[b]No resonance in these coupled channels.

D-wave scattering phase shifts with a narrow width. Also, the coupling pushes down the energy of the dibaryon a little. The $N\Xi^*$, $\Sigma\Sigma^*$, and $\Sigma^*\Sigma^*$ three-bound-state coupling pushes the lowest state down to 2425 MeV. The open channel, D-wave $\Lambda\Lambda$ coupling pushes down the state 1 MeV further. However, except for the lowest state $N\Xi^*$, other resonances that might be related to excited states $\Sigma\Sigma^*$ and $\Sigma^*\Sigma^*$ do not clearly show up in the $\Lambda\Lambda$ D-wave phase shifts in the four-channel coupling calculation. There is only a wavy motion around the energy of the second state, $\Sigma\Sigma^*$. The reason may be the opening of $N\Xi^*$, which pushes up those otherwise excited resonances.

The phase-shift calculation of D-wave $N\Xi$ gives similar results to those of the $\Lambda\Lambda$ calculation. So the dibaryon resonance has almost the same behavior on different scattering channels. Summing up the two decay widths, we have that the dibaryon state with $I, J = 0, 2$ has a total decay width of 3.4 MeV, and the width increases to 11 MeV after taking into account the off-shell width of Ξ^*.

In the ChQM, we obtained almost the same results as in the QDCSM. So it is a promising approach to look for a dibaryon state with quantum numbers $I, J = 0, 2$ in the scattering of $N\Xi$ with the J-PARC Ξ beam in the near future.

In the same strangeness sector, the states with $I, J = 1, 3$ are also interesting. In the QDCSM, there are two decuplet-decuplet bound states $\Delta\Xi^*$ and $\Sigma^*\Sigma^*$, whereas there is only one bound state $\Delta\Xi^*$ in the ChQM. The results are shown in Table V and Figs. 7–9. The possible two-body decay channels are $N\Xi$, $\Lambda\Sigma$, $\Sigma\Sigma$, $N\Xi^*$, $\Delta\Xi$, and $\Sigma\Sigma^*$. The situation is the same as before: the bound states appear as narrow resonances after coupling to the D-wave open channels by tensor interaction, and the energies are pushed down a little. From Figs. 7–9, we find that there is only one resonance in the octet-octet baryon scattering, although there are two bound states in the QDCSM. The reason is that the channel coupling pushes the higher state above the threshold. The cusps

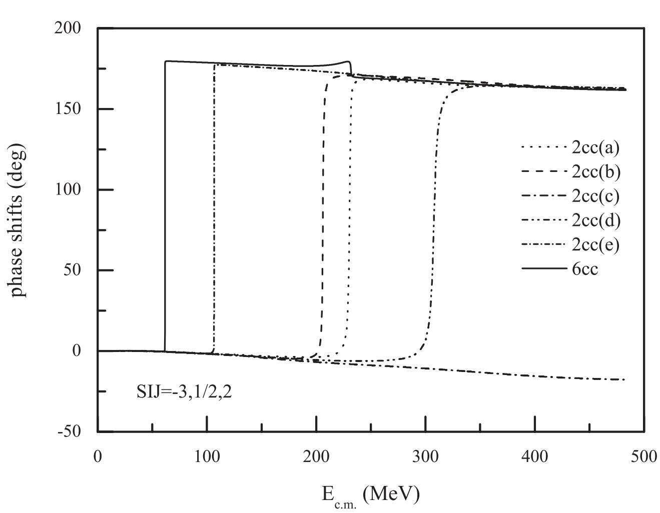

FIG. 10. The D-wave $\Lambda\Xi$ phase shifts with $I, J = 1/2, 2$ in QDCSM. 2cc(a), 2cc(b), 2cc(c), 2cc(d), and 2cc(e) stand for $\Lambda\Xi$ coupling to $\Sigma\Xi^*$, $\Xi\Sigma^*$, $\Lambda\Xi^*$, $\Sigma^*\Xi^*$, and $N\Omega$. The six-channel coupling is denoted by 6cc.

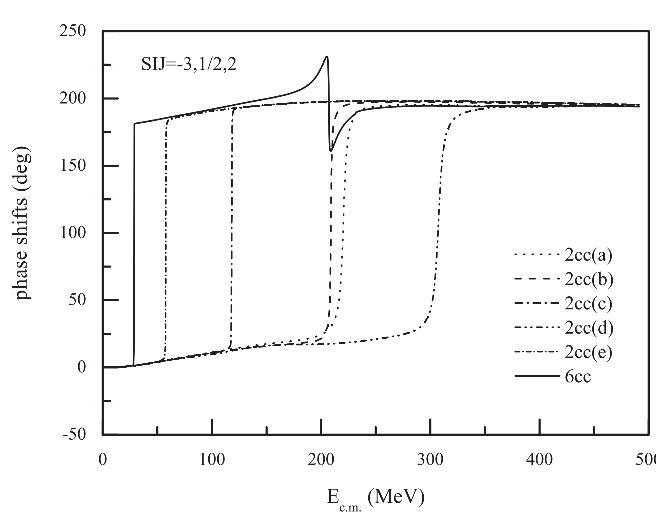

FIG. 11. Same as Fig. 10 in the ChQM.

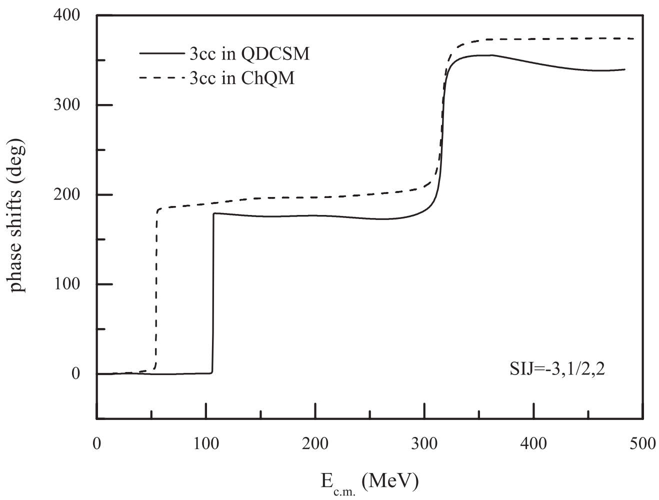

FIG. 12. The D-wave $\Lambda\Xi$ phase shifts with $I, J = 1/2, 2$, including $N\Omega$ and $\Sigma^*\Xi^*$ channels.

in the curves denoted by 2cc(b) are a remnant of $\Sigma^*\Sigma^*$ in the ChQM. So these two quark models both support that there is a $I, J = 1, 3$ dibaryon resonance with a mass of around 2627 (2661) MeV and a width of around 50 (90) MeV in the QDCSM (ChQM).

The ΞN scattering measurement, if it is done at J-PARC, should be extended to this resonance energy region.

(iii) $S = -3$. $N\Omega$ is an interesting state in this section. It has been proposed that $N\Omega$ is a good dibaryon candidate [5,7]. This state can serve as a test of the flavor-dependent q-q interaction due to Goldstone-boson exchange and due to quark delocalization, because there is no common flavor quark between N and Ω and so no quark exchange between these two baryons. In this calculation, the single-channel approximation gives three bound states, $\Sigma\Xi^*$, $\Xi\Sigma^*$, and $\Sigma^*\Xi^*$, in the QDCSM and five bound states, $N\Omega$, $\Sigma\Xi^*$, $\Xi\Sigma^*$, $\Lambda\Xi^*$, and $\Sigma^*\Xi^*$, in the ChQM with quantum numbers $I, J = 1/2, 2$. In the QDCSM, the adiabatic calculation of $N\Omega$ with the new color screening parameter shows that there is only a weak attraction ($\sim$12 MeV) between N and Ω. The dynamical calculation did not yield a bound $N\Omega$ state. However, coupling to the open-channel D-wave $\Lambda\Xi$ pushes the $N\Omega$ state below the threshold to form a resonance at 2592 MeV with a very narrow width of 10 keV. The results are shown in Table VI and Figs. 10 and 11. By coupling all the states together, only one resonance appears at 2547 MeV, and a wavy motion appears around 2700 MeV.

A methodology study of the channel coupling phase-shift calculation has been done with these channels. We first do a three-channel, $\Lambda\Xi$, $N\Omega$, $\Sigma^*\Xi^*$, coupling calculation. The energy of $N\Omega$ is significantly smaller than that of $\Sigma^*\Xi^*$, and so the coupling between these two channels is rather weak. The result is shown in Fig. 12, which shows that there are two resonances in the $\Lambda\Xi$ D-wave phase shifts, located at 2588 and 2797 MeV, respectively. In comparison with $N\Omega$-$\Lambda\Xi$, $\Sigma^*\Xi^*$-$\Lambda\Xi$ two-channel calculations, there are 2- and 5-MeV changes for $N\Omega$ and $\Sigma^*\Xi^*$, respectively. The decay widths of the two resonances, $\sim$10 keV and 5 MeV, also show that these two resonances come from $N\Omega$ and $\Sigma^*\Xi^*$. However, a six-channel calculation does not show more than one complete resonance. To check this multiresonance behavior, the same calculation has been done for the ChQM. We obtain the same results (see Table VI and Figs. 11 and 12). Usually the lowest state will be pushed down by more channels coupling, but whether the other states move up or down is dependent on the details of these coupling channels. Here the other states are pushed up from three- to six-channel coupling.

The conclusion of these two quark model calculations is the existence of a very narrow (of width less than 4 MeV) $I, J = 1/2, 2$ dibaryon resonance with a mass of 2547 MeV (QDCSM) or 2528 MeV (ChQM). This conclusion is different from that of Oka [4] and in agreement with Silvestre-Brac and Leandri [39] and our previous results [5,7].

This resonance might be detected in relativistic heavy ion collisions by the existing RHIC and COMPAS detectors through the reconstruction of the $\Lambda\Xi$ vertex mass.

TABLE VII. The mass and width of state $S, I, J = -3, 3/2, 3$, in MeV. The theoretical thresholds of the two channels $\Sigma^*\Xi^*$ and $\Delta\Omega$ are 2857 and 2886 MeV in the QDCSM and 2856 and 2874 MeV in the ChQM, respectively.

Coupling channels	QDCSM			ChQM		
	M	Γ	Γ_{bs}	M	Γ	Γ_{bs}
$\Sigma^*\Xi^*$	2822	–	–	2836	–	–
$\Delta\Omega$	2836	–	–	2851	–	–
$\Sigma^*\Xi^*$-$\Delta\Omega$	2797	–	–	2791	–	–
$\Sigma^*\Xi^*$-$\Sigma\Xi$	2821	2.9	28.2	2836	4.8	35.0
$\Delta\Omega$-$\Sigma\Xi$	2835	2.7	68.3	2849	4.7	87.7
$\Sigma^*\Xi^*$-$\Delta\Omega$-$\Sigma\Xi$	2795	2.3	47.5	2788	6.1	52.4
$\Sigma^*\Xi^*$-$\Sigma^*\Xi$	2821	0.07	30.1	2837	0.2	37.2
$\Delta\Omega$-$\Sigma^*\Xi$	2835	0.004	70.9	2849	0.01	90.8
$\Sigma^*\Xi^*$-$\Delta\Omega$-$\Sigma^*\Xi$	2796	0.02	51.4	2790	0.03	56.7
$\Sigma^*\Xi^*$-$\Sigma\Xi^*$	2821	0.001	30.3	2838	0.001	37.2
$\Delta\Omega$-$\Sigma\Xi^*$	2835	0.009	71.0	2850	0.009	92.2
$\Sigma^*\Xi^*$-$\Delta\Omega$-$\Sigma\Xi^*$	2796	0.02	52.4	2791	0.01	57.7

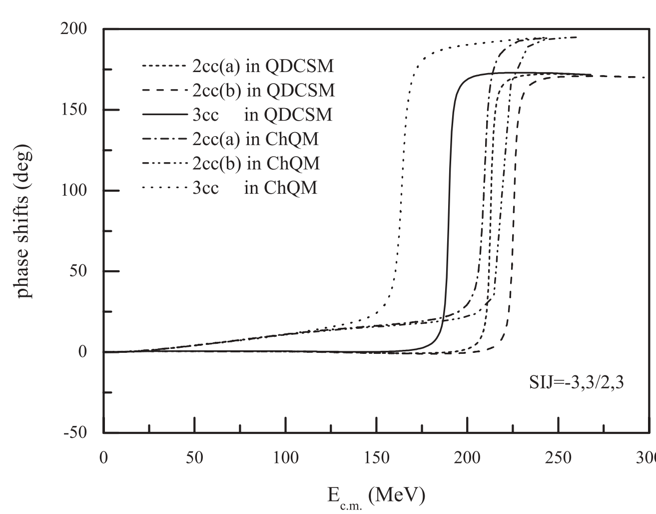

FIG. 13. The D-wave $\Sigma\Xi$ phase shifts with $I, J = 3/2, 3$. 2cc(a) and 2cc(b) stand for $\Sigma\Xi$ coupling to $\Sigma^*\Xi^*$ and $\Delta\Omega$, respectively, and the three-channel coupling is denoted by 3cc.

TABLE VIII. The mass and width of state $S, I, J = -5, 1/2, 0$ in MeV. The theoretical threshold of channel $\Xi^*\Omega$ is 3153 MeV in the QDCSM and 3138 MeV in the ChQM, respectively.

Coupling channels	QDCSM			ChQM		
	M	Γ	Γ_{bs}	M	Γ	Γ_{bs}
$\Xi^*\Omega$	nb[a]	–	–	3097	–	–
$\Xi^*\Omega$-$\Xi\Omega$	nr[b]	–	–	3095	0.2	5.3

[a]Unbound.
[b]No resonance in these coupled channels.

In the same strangeness sector, the system $I, J = 3/2, 3$ is also interesting. There are two decuplet-decuplet channels: $\Sigma^*\Xi^*$ and $\Delta\Omega$. The calculated results are shown in Table VII, and the corresponding octet-octet baryons $\Sigma\Xi$ scattering phase shifts are shown in Fig. 13. The QDCSM suggests a dibaryon resonance with a mass of 2795 MeV and a width of 50 MeV, and the ChQM gives the resonance at 2788 MeV with a width of about 60 MeV. If the $\Lambda\Xi$ vertex mass is successfully reconstructed at RHIC and COMPAS, then it is interesting to reconstruct the $\Sigma\Xi$ vertex mass.

(iv) $S = -4$. In this section, neither the QDCSM nor the ChQM have a dibaryon resonance.

(v) $S = -5$. For the system $I, J = 1/2, 0$, there is a mild attraction between Ξ^* and Ω. In the QDCSM, the attraction ($\sim$28 MeV) is not strong enough to bind the two baryons, while in the ChQM the attraction ($\sim$40 MeV) is just enough to form a bound state. Since the spin is zero, the decuplet-decuplet state $\Xi^*\Omega$ can only couple to $\Xi\Omega$ through tensor interaction. In the D-wave phase shifts of $\Xi\Omega$ scattering, the state $\Xi^*\Omega$ appears as a cusp at the threshold of $\Xi^*\Omega$ in the QDCSM and appears as a narrow (with a width of 0.2 MeV) resonance at 3095 MeV in the ChQM (see Table VIII and Fig. 14). Taking into account the off-shell width of Ξ^* ($\Gamma_{bs} = 5.3$ MeV), one finds that the width of the state $\Xi^*\Omega$ is about 5.5 MeV.

(vi) $S = -6$. The di-Ω with $I, J = 0, 0$ was reported as a strong-interaction-stable state [36]. There is no other dibaryon resonance in this sector.

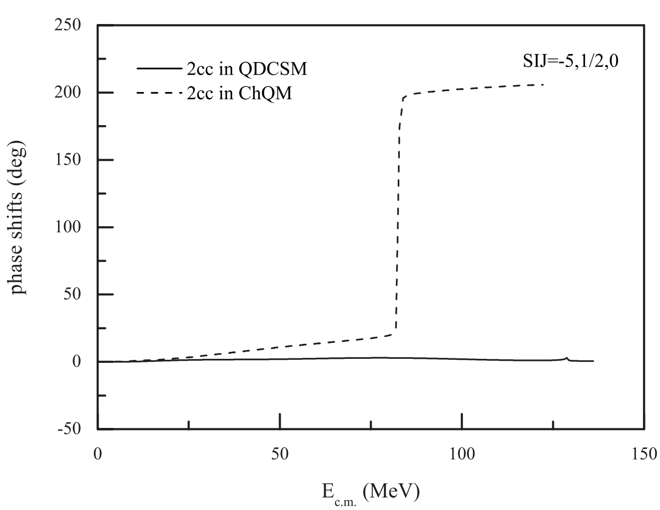

FIG. 14. The D-wave $\Xi\Omega$ phase shifts with $I, J = 1/2, 0$. 2cc denotes the coupling $\Xi^*\Omega$-$\Xi\Omega$.

IV. CONCLUSION

In this paper, we performed a channel coupling scattering calculation with the inclusion of possible dibaryon states in the framework of RGM by means of two constituent quark models, in which the baryons are treated as three-quark clusters. Because the RGM formalism cannot reproduce the measured baryon masses, the RGM must be modified to fit the scattering kinematics. A simple prescription, which has been used in other calculations, is applied.

The two quark models have been successfully applied to fit NN scattering phase shifts, deuteron properties, $N\Sigma$ and $N\Lambda$ scattering, and reaction cross sections with the unified parameters. Even though they have different mechanisms of intermediate-range attraction, the two quark models give almost the same dibaryon resonances. This is a further check of the equivalence of the intermediate-range attraction mechanism, the quark delocalization color screening mechanism in the QDCSM and the σ meson exchange in the ChQM. Before coupling to the open scattering channel the dibaryon state appears as a bound state. After coupling it appears as a resonance in the corresponding baryon-baryon scattering. The location of the resonance is generally different from the energy of the stand-alone bound state due to the well-known energy shift. In the case of the S-wave bound-state coupling to the S-wave baryon-baryon scattering channel, the energy shifts will be as large as 200 or 300 MeV [31]. In the present calculation, all couplings are due to tensor interaction, the S-wave bound states coupling to D-wave baryon-baryon scattering channels. So the energy shifts are small, usually a few MeV. In addition, these resonances will acquire a small width (a few MeV or less). However, as we are dealing with strong-interaction-unstable baryons, the decay width of these baryons should be taken into account. We use a simple estimation developed in [31] to obtain the off-shell width due to binding. The widths of dibaryon resonances usually increase to tens of MeV.

In our calculation we found an interesting phenomenon: For a fixed bound state, the coupling of different baryon-baryon scattering channels give almost the same resonance energy. If there are several bound states with the same quantum numbers, the scattering channel coupling generally only generates one complete resonance, the lowest dibaryon state. Other states do not appear as resonances in the baryon-baryon scattering phase shifts due to the interaction between these coupling channels. We are not sure if this is a special case for our studied channels. Further study is needed.

Based on our calculation, we suggest that the following dibaryon resonances are worth searching for through YN scattering when the hyperon beams are available or through reconstruction of the multistrangeness vertex masses with data already stored in the detectors of the relativistic heavy ion collisions: (1) $S, I, J = -1, 1/2, 3$, with a mass of 2440–2540 MeV and a width of 48–118 MeV through $N\Lambda$ or $N\Sigma$ scattering; (2) $S, I, J = -2, 0, 2$, with a mass of 2400–2430 MeV and width of 10–11 MeV through $N\Xi$ scattering; (3) $S, I, J = -2, 1, 3$, with a mass of 2620–2660 MeV and a width of 50–90 MeV through $N\Xi$ scattering; (4) $S, I, J = -3, 1/2, 2$, with a mass of 2528–2547 MeV and a width of 2–4 MeV through $\Lambda\Xi$ mass vertex reconstruction; and (5) $S, I, J = -3, 3/2, 3$, with a mass of 2788–2795 MeV and a width of 50–60 MeV through $\Sigma\Xi$ vertex mass reconstruction. These two quark models have been fitted to vast NN data and a small amount of $N\Lambda$, $N\Sigma$ scattering data. So these predictions are more reliable for low-strangeness channels.

ACKNOWLEDGMENTS

This work is supported partly by the National Science Foundation of China under Contract Nos. 10775072, 10947160 and the Research Fund for the Doctoral Program of Higher Education of China under Grant No. 20070319007.

[1] R. L. Jaffe, Phys. Rev. Lett. **38**, 195 (1977).
[2] R. L. Jaffe, Phys. Rep. **409**, 1 (2005) and references therein.
[3] M. Oka, K. Shimizu, and K. Yazaki, Nucl. Phys. A **464**, 700 (1987).
[4] M. Oka, Phys. Rev. D **38**, 298 (1988).
[5] T. Goldman, K. Maltman, G. J. Stephenson, K. E. Schmidt, and F. Wang, Phys. Rev. Lett. **59**, 627 (1987).
[6] F. Wang, J. L. Ping, G. H. Wu, L. J. Teng, and T. Goldman, Phys. Rev. C **51**, 3411 (1995).
[7] H. R. Pang, J. L. Ping, F. Wang, T. Goldman, and E. G. Zhao, Phys. Rev. C **69**, 065207 (2004); H. R. Pang, J. L. Ping, L. Z. Chen, and F. Wang, Chin. Phys. Lett. **21**, 1455 (2004).
[8] Q. B. Li and P. N. Shen, Eur. Phys. J. A **8**, 417 (2000).
[9] T. Goldman, K. Maltman, G. J. Stephenson, K. E. Schmidt, and F. Wang, Phys. Rev. C **39**, 1889 (1989).
[10] J. L. Ping, H. R. Pang, F. Wang, and T. Goldman, Phys. Rev. C **65**, 044003 (2002).
[11] J. L. Ping, F. Wang, and T. Goldman, Nucl. Phys. A **688**, 871 (2001).
[12] V. B. Kopeliovich, B. Schwesinger, and B. E. Stern, Phys. Lett. B **242**, 145 (1990).
[13] V. B. Kopeliovich, Nucl. Phys. A **639**, 75c (1998).
[14] Z. Y. Zhang, Y. W. Yu, C. R. Ching, T. H. Ho, and Z. D. Lu, Phys. Rev. C **61**, 065204 (2000).
[15] Q. B. Li, P. N. Shen, Z. Y. Zhang, and Y. W. Yu, Nucl. Phys. A **683**, 487 (2001).
[16] M. Bashkanov *et al.* (CELSIUS-WASA Collaboration), Phys. Rev. Lett. **102**, 052301 (2009).
[17] B. Aubert *et al.* (BABAR Collaboration), Phys. Rev. Lett. **90**, 242001 (2003).
[18] S. K. Choi *et al.* (BABAR Collaboration), Phys. Rev. Lett. **91**, 262001 (2003).
[19] A. V. Evdokimov *et al.* (SELEX Collaboration), Phys. Rev. Lett. **93**, 242001 (2004).
[20] J. Z. Bai *et al.* (BES Collaboration), Phys. Rev. Lett. **91**, 022001 (2003).
[21] N. Ishii, S. Aoki, and T. Hatsuda, Phys. Rev. Lett. **99**, 022001 (2007).
[22] C. Alexandrou, P. de Forcrand, and A. Tsapalis, Phys. Rev. D **65**, 054503 (2002); T. T. Takahashi, H. Suganuma, Y. Nemoto, and H. Matsufuru, *ibid.* **65**, 114509 (2002).
[23] F. Okiharu, H. Suganuma, and T. T. Takahashi, Phys. Rev. Lett. **94**, 192001 (2005).
[24] Y. Fujiwara, C. Nakamoto, and Y. Suzuki, Phys. Rev. Lett. **76**, 2242 (1996); Y. W. Yu, Z. Y. Zhang, P. N. Shen, and L. R. Dai, Phys. Rev. C **52**, 3393 (1995).
[25] A. Valcarce, H. Garcilazo, F. Fernández, and P. Gonzalez, Rep. Prog. Phys. **68**, 965 (2005) and references therein.
[26] N. Kaiser, S. Grestendorfer, and W. Weise, Nucl. Phys. A **637**, 395 (1998); E. Oset, H. Toki, M. Mizobe, and T. T. Takahashi, Prog. Theor. Phys. **103**, 351 (2000); M. M. Kaskulov and H. Clement, Phys. Rev. C **70**, 014002 (2004).
[27] F. Wang, G. H. Wu, L. J. Teng, and T. Goldman, Phys. Rev. Lett. **69**, 2901 (1992); G. H. Wu, L. J. Teng, J. L. Ping, F. Wang, and T. Goldman, Phys. Rev. C **53**, 1161 (1996).
[28] G. H. Wu, J. L. Ping, L. J. Teng, F. Wang, and T. Goldman, Nucl. Phys. A **673**, 279 (2000).
[29] L. Z. Chen, H. R. Pang, H. X. Huang, J. L. Ping, and F. Wang, Phys. Rev. C **76**, 014001 (2007).
[30] M. Kamimura, Prog. Theor. Phys. Suppl. **62**, 236 (1977).
[31] J. L. Ping, H. X. Huang, H. R. Pang, F. Wang, and C. W. Wong, Phys. Rev. C **79**, 024001 (2009).
[32] D. R. Entem, F. Fernandez, and A. Valcarce, Phys. Rev. C **62**, 034002 (2000).
[33] F. Fernandez, A. Valarce, U. Straub, and A. Faessler, J. Phys. G **19**, 2013 (1993).
[34] J. Vijande, F. Fernandez, and A. Valcarce, J. Phys. G **31**, 481 (2005).
[35] Y. Fujiwara, M. Kohno, C. Nakamoto, and Y. Suzuki, Prog. Theor. Phys. **104**, 1025 (2000); Y. Fujiwara, Y. Suzuki, and C. Nakamoto, Prog. Part. Nucl. Phys. **58**, 439 (2007).
[36] M. Chen, F. Gong, H. X. Huang, and J. L. Ping, Mod. Phys. Lett. A **25**, 1603 (2010).
[37] B. Julia-Diaz, T. -S. H. Lee, A. Matsuyama, and T. Sato, Phys. Rev. C **76**, 065201 (2007).
[38] D. R. Entem, F. Fernandez, and A. Valcarce, Phys. Rev. C **67**, 014001 (2003).
[39] B. Silvestre-Brac and J. Leandri, Phys. Rev. D **45**, 4221 (1992).